Published in final edited form as:
*Neuron*. 2011 February 24; 69(4): 805–817. doi:10.1016/j.neuron.2011.01.012.

# Dual mechanism of neuronal ensemble inhibition in primary auditory cortex

**M.N O'Connell**[1,2], **A Falchier**[1], **T McGinnis**[1], **C.E Schroeder**[1,3], and **P Lakatos**[1,4]

[1] Cognitive Neuroscience and Schizophrenia Program, Nathan Kline Institute, Orangeburg, New York 10962

[2] Program in Cognitive Neuroscience, City College CUNY, New York, New York 10031

[3] Department of Psychiatry, Columbia College of Physicians and Surgeons, New York, New York 10032

[4] Department of Psychiatry, New York University School of Medicine, New York, New York 10016

## SUMMARY

Inhibition plays an essential role in shaping and refining the brain s representation of sensory stimulus attributes. In primary auditory cortex (A1), so-called "sideband" inhibition helps to sharpen the tuning of local neuronal responses. Several distinct types of anatomical circuitry could underlie sideband inhibition, including direct thalamocortical (TC) afferents, as well as indirect intracortical mechanisms. The goal of the present study was to characterize sideband inhibition in A1 and to determine its mechanism by analyzing laminar profiles of neuronal ensemble activity. Our results indicate that both lemniscal and non-lemniscal TC afferents play a role in inhibitory responses via feed-forward inhibition and oscillatory phase reset respectively. We propose that the dynamic modulation of excitability in A1 due to the phase reset of ongoing oscillations may alter the tuning of local neuronal ensembles and can be regarded as a flexible overlay upon the more obligatory system of lemniscal feed-forward type responses.

## INTRODUCTION

Frequency based encoding is a fundamental feature of the auditory system, starting with the spatial ordering of frequency selectivity along the cochlea and continuing with spatially ordered projections and topographically organized frequency maps even beyond primary cortical areas (Merzenich and Brugge, 1973; Kosaki et al., 1997; Kaas and Hackett, 2000). The prevalence of frequency based maps in the auditory system suggests that the extraction of information contained in the frequency content of auditory stimuli is essential for perception and sensory guided behavior. The fact that non-primary auditory areas surrounding primary cortical fields have degraded topographical frequency representations (Kaas and Hackett, 2000) seems to suggest that primary cortical areas play a crucial role in the frequency based computation of auditory representations, since topographically organized feature maps are thought to enhance the efficiency of feature based computations in sensory systems (Kaas, 1997).

Corresponding author: Peter Lakatos, M.D., Ph.D., Cognitive Neuroscience and Schizophrenia Program, Nathan S. Kline Institute for Psychiatric Research, plakatos@nki.rfmh.org.

The orderly and progressive spatial arrangement of tone frequency neural representations (tonotopic map) is achieved by activation through direct, spatially organized thalamocortical (TC) inputs from the ventral subdivision of the medial geniculate nucleus (MGNv) of the thalamus (Huang and Winer, 2000; Lee et al., 2004; Liu et al., 2007). However it has been shown that anatomical projections from MGN to auditory cortex are not organized in a simple point-to-point fashion, as A1 neurons receive converging inputs from MGN neurons tuned to several 'neighboring frequencies' surrounding their best frequency (BF) (Miller et al., 2001; Lee et al., 2004; Winer and Lee, 2007). This predicts that the frequency tuning of A1 should be less sharp than that of MGN, which is not the case (Creutzfeldt et al. 1980; Miller et al., 2002). Hence it has been proposed that intracortical inhibition functions to sharpen the broader pure-tone evoked excitation in A1 in order to enhance response contrast of the neural representation of frequency (Shamma and Symmes, 1985; Suga, 1995; Sutter et al., 1999). This proposition has been supported by pharmacological experiments showing that the blocking of cortical GABA-mediated inhibition results in a reduction of frequency selectivity in the auditory cortex (Wang et al., 2000; Foeller et al., 2001). In addition to electrophysiological studies, fMRI (Tanji et al., 2010) and optical imaging studies (Horikawa et al., 1996) also indicate suppression of neural activity in response to tones whose neural frequency representation lies in proximity to the BF in a given region of A1 (sideband inhibition). Recent studies have shown that inhibition in A1 can be modulated depending on task demands (Fritz et al., 2003, 2005), and can be plastically modified so that A1 is preferentially responsive to behaviorally relevant stimuli (Recanzone et al., 1993; Galindo - Leon et al., 2009).

Although it is apparent from these studies that sideband inhibition in the auditory cortex is necessary for the adaptive processing of behaviorally-relevant, frequency-specific properties of an acoustic stimulus, its precise mechanism has not yet been established. In A1, as in primary somatosensory (e.g. Swadlow et al., 2002; Cruikshank et al., 2007) and visual cortices (e.g. Ferster 1988; Krukowski and Miller 2001), two types of inhibition provide potential substrates for this effect: 1) feed-forward inhibition mediated by TC afferents from MGNv centered on the granular layer (Wehr and Zador, 2003, 2005; Zhang et al., 2003; Tan et al., 2004; Wu et al., 2008), and 2) lateral type inhibition mediated by intracortical connections that are weighted towards the extragranular layers (Kurt et al., 2008; Moeller et al., 2010). Besides these lemniscal TC and intracortical routes, non-lemniscal TC afferents (Jones et al., 1998) have also been implicated in modulating the excitability of neuronal ensembles in A1 (Lakatos et al., 2007; 2009). These non-specific inputs target mainly the supragranular layers, and seem to be under top-down control. The suggested mechanism underlying this type of modulation is the reset of ongoing neuronal oscillations (Sayers et al., 1974; Makeig et al., 2004; Lakatos et al., 2009). Since these oscillations reflect the net fluctuation of excitability in a local neuronal ensemble (reviewed by Young and Eggermont, 2009), reset to their high excitability phase produces facilitation of responses to coincident auditory input, while reset to their low excitability phase can produce a suppression of auditory responses (Lakatos et al., 2007). While the proposed role of the first two types of inhibition in A1 is the sharpening of response timing and frequency tuning, the role of non-specific TC inputs appears to be the dynamical control of cortical excitability based on bottom up and top down influences, and a matching of cortical oscillatory rhythms to those present in task-relevant stimulus streams (Lakatos et al., 2008; Schroeder and Lakatos 2009). It is not known whether the frequency content of auditory stimuli can change the sign of oscillatory phase reset, and thus whether modulation of neuronal oscillations plays a role in the frequency tuning of A1.

The purpose of this study was twofold: 1) to characterize inhibitory responses to pure tones in A1 in laminar profiles of neuronal ensemble activity, and 2) to examine whether using laminar recordings we could determine which of the above described three mechanisms

could play a role in sideband inhibition. We analyzed laminar current source density (CSD) and multiunit activity (MUA) profiles sampled during multielectrode penetrations of A1 in awake macaque monkeys (*Macacca mulatta*) in response to different frequency pure tones. CSD profiles coupled with the firing of the local neuronal ensemble (MUA) are an invaluable tool in distinguishing between excitatory and inhibitory conductances underlying field potentials, since they provide a reliable index of the location and direction of transmembrane current flow (Mitzdorf, 1985; Schroeder et al., 1998). Also, CSD analysis provides a sensitive measure of synaptic activity even in cases of subthreshold, modulatory responses like oscillatory phase reset (see above). Because our recordings sample all layers simultaneously, we can define and quantify laminar activation profiles, thus generating evidence regarding the relative contributions of lemniscal and extralemniscal thalamic inputs, as well as corticocortical inputs (Schroeder et al., 2003). We found evidence that while specific feedforward TC afferents play a role in both excitatory and inhibitory neuronal ensemble responses, ongoing oscillatory activity is also modulated in a frequency specific manner by oscillatory phase reset, and the two types of responses are independent of each other. This layered modulation of excitability in A1 provides a great opportunity for the top down orchestration of excitability across neuronal ensembles processing different frequencies, so that this cortical area can serve as a complex spectro-temporal filter in the processing of behaviorally relevant acoustic information.

## RESULTS

In the present study we analyzed laminar CSD and MUA profiles of responses to pure tones ranging from 353.5 Hz to 32 kHz in half octave intervals obtained with linear array multicontact electrodes from 64 sites in 9 awake macaque monkeys. The sites were distributed evenly along the tonotopic axis of primary auditory cortex, with best frequencies (BF) ranging from ~0.3 kHz to 32 kHz. In addition to the typical excitatory response to BF tones signaled by a phasic-tonic increase of cell firing (Figure 1C top), similar to previous studies (e.g. Sutter et al., 1999; Lakatos et al., 2005a; Steinschneider et al., 2008), most A1 sites responded with a suppression of MUA, signaling inhibition, to at least one of the pure tones presented at 60 dB SPL in our suprathreshold tonotopy paradigm (see experimental procedures). We found that 78% of sites (50/64) showed significant post stimulus (15 – 40 ms) MUA suppression compared to baseline (−50 – 0 ms) to at least one of the pure tones presented (dependent t-test, $p < 0.01$). The sites that did not show significant post-stimulus suppression were excluded from further analysis.

### Properties of MUA Suppression in Inhibitory Sidebands

Since the suppression of post-stimulus MUA was largest in the granular layer in the case of all inhibitory type responses to pure tones (Tukey s test, $p < 0.01$), we first decided to analyze granular layer MUA responses. As Figure 1B illustrates, we noted that inhibition could occur either in response to tones whose frequency was higher (InhibHi, n = 19), lower (InhibLo, n = 17) or both higher and lower (InhibHi&Lo, n = 14) than the BF of a site. These sites were evenly distributed between monkeys. The sites with inhibitory response to higher frequency tones had a low BF (0.3–4 kHz), while the BF of sites with inhibitory responses to low frequency tones was generally high (8–32 kHz). Sites that responded with inhibition to both low and high frequency tones had an intermediate BF (4–16 kHz). While the frequency difference between BF and inhibitory tones was two octaves on average in the InhibHi (mean = 2 octaves, SD = 0.9), and InhibLo groups (mean = 2.3 octaves, SD = 0.88), the average frequency difference between BF tone and maximal inhibition was about half that in the InhibHi&Lo group, on average 1.1 octaves (SD = 0.59), indicating that sites comprising this group were the most sharply tuned (Fig. 1B). While intriguing, this result

could be at least partially due to the relatively sparse sampling of frequencies across seven octaves in our experiments.

Figure 2A shows that there is a significant difference between the pooled best frequencies of the three groups while inhibitory frequencies have considerable overlap. As a consequence, there is also a clear difference of MUA response onset latency to BF tones between the inhibitory groups (Fig 2B), since it has been shown that response onset latency to BF tones depends on their frequency (Mendelson et al., 1997; Kaur et al., 2004; Lakatos et al., 2005a). The InhibLo group (highest BF) has the earliest response onset latency (BF3, mean = 7.7ms, SD = 1.0), the next earliest is the InhibHi&Lo group (BF2, mean = 8.3ms, SD = 0.95) and the group with the longest BF tone related MUA response onset latency is the InhibHi group (BF1, mean = 11.9ms, SD = 2.8). The response onset in this last group occurred significantly later than BF related MUA onset latencies of the other two groups (Tukey's test, $p < 0.01$).

The lower part of Figure 2B shows the pooled granular MUA onset latencies of the inhibitory responses in the four inhibitory sidebands (the InhibHi&Lo group has two inhibitory sidebands). While there was an apparent frequency dependence of response onset latencies similar to the pooled BF responses, onset latencies of the inhibitory sidebands did not differ significantly from one another (Kruskal-Wallis test, $p > 0.01$), which is not surprising, since the pooled frequencies of the inhibitory sidebands have considerable overlap (Fig. 2A). It is also apparent from Figure 2B that while the onset of excitatory (in response to BF tone) and corresponding inhibitory responses in the InhibLo and InhibHi&Lo groups are significantly different (inhibition occurs significantly later) there is no significant difference between the onset of excitation and inhibition in the InhibHi group. The consequence of this can be seen in Figure 1C on the bottom: while in the former two groups (InhibLo and InhibHi&Lo) there is an excitatory MUA spike (excitatory since in laminar CSD profiles it was paired with a sink) before the inhibition occurs, in the InhibHi group excitation is completely abolished by concurrently occurring inhibition.

The initial excitatory response to tones that result in significant inhibition is probably due to a spread of activation across BF representations in the cochlea and corresponding TC afferents by the relatively high intensity sounds (60 dB SPL) used here (Aitkin and Webster, 1972); the effect emerges in the higher frequency representations of A1 because of the latency advantage of high frequency excitatory responses compared to low frequency inhibitory ones. This short (about 5 ms) excitatory MUA component was present in 14 out of 17 inhibitory responses in the InhibLo group, 9 out of 14 recordings in the lower inhibitory sideband, and in 5 out of 14 recordings in the upper inhibitory sideband of the InhibHi&Lo group. The initial excitation was absent (0/19) in the InhibHi group. We also determined the timing of maximal granular MUA inhibition among the 4 different inhibitory sub-groupings, which was not significantly different between groups (Kruskal-Wallis test, $p > 0.01$): it occurred on average at 23.4 ms after stimulus onset.

Since one of the mechanisms that has been proposed to underlie off responses in auditory cortex is a rebound from inhibition, we decided to analyze off responses following on responses with largest excitation (BF) and inhibition (non-BF). The rationale was that if this was the case, off responses should be absent following excitatory responses to BF tones, and we should find an off response following most inhibitory responses. First we determined whether granular layer MUA was significantly above baseline following the offset of pure tones in the 115–140 ms time interval (15–40 ms post-offset), and next we verified that the above baseline MUA is not due to a "lingering" of the sustained on response, but rather is a consequence of a phasic MUA increase. We found that 18 out of 50 BF responses (36%) and 22 out of 64 non-BF responses (34%) were followed by an excitatory off response. This

indicates that rather than being merely a consequence of the on response, off responses might be driven by inputs that are distinct from the ones activated by sound onset, with mostly nonoverlapping tuning, as suggested by a recent study (Scholl et al., 2010).

## Laminar Profiles of BF vs. non-BF Inhibitory Responses in A1

After functionally identifying cortical layers in each experiment, we compared MUA and CSD laminar response profiles to BF tones and to tones that resulted in the largest inhibition (Fig. 3). While BF tones in all 3 groups resulted in a significant MUA increase in all layers, inhibitory responses were signaled by decreased MUA (examples of a low and high BF site (from the InhibHi and InhibLo groups respectively) are shown in Fig. 3A). The post-stimulus MUA change compared to baseline was largest in the granular layers in both cases. Analysis of the corresponding CSD profiles in all experiments revealed that as previously described (e.g. Schroeder et al., 2003;Lakatos et al., 2007;Steinschneider et al., 2008) the BF tone produces activation of all cortical layers with initial postsynaptic response, a current sink with concomitant increase in neuronal firing in layer 4, followed by later responses in extragranular layers. This sequence of activation, coupled with a source (net outward transmembrane current flow) over sink (net inward transmembrane current flow) in the supragranular layers is typical of an excitatory "feedforward" or "driving" type activation profile (Fig. 3B, left panels).

In contrast to these types of responses, we found that inhibitory responses were of much lower amplitude (note the different scales in Fig. 3B), and that the pattern of sinks and sources in the supragranular layer was inverted in the inhibitory responses compared to excitatory BF responses. The inverted current flow in all cortical layers reflected by the inverted CSD profiles compared to excitatory profiles suggests that inhibition to non-BF pure tones occurs in all cortical layers simultaneously. This was characteristic of all 50 A1 sites analyzed; however in some cases (in the InhibLo and InhibHi&Lo groups) the granular source associated with the inhibitory responses was preceded by a short sink concomitant with the excitatory MUA spike preceding MUA suppression (see above). In addition to an inverted sink-source pattern, another key difference between the BF and non-BF response profiles is that, while the onset of excitatory BF responses is significantly earlier in granular than in supragranular layers (Wilcoxon signed rank, $p < 0.01$) typical of a feedforward type sequential activation of cortical layers, non-BF responses occur at roughly the same time in granular and supragranular layers (Fig. 4). This suggests that the activation of supragranular layers in the case of responses to non-BF tones may not result solely from a hierarchical interlaminar spread of activation. Rather, this type of laminar response onset profile indicates the influence of TC inputs that target the upper layers (non-lemniscal TC inputs), or horizontal inputs from other regions of A1. Further experimentation will be necessary to clarify this issue.

## The Physiological Mechanism of the Inhibitory CSD Response

The purpose of our next set of analysis was to determine the mechanism of the inhibitory CSD response. We wanted to see if we could establish whether inhibition is dominated by an evoked type response characterized by a stimulus related CSD amplitude increase in single trials as in the case of BF responses (Lakatos et al., 2007, 2009), or a reorganization of ongoing oscillatory activity (phase reset). As a first step, we calculated single trial laminar CSD analytic amplitudes and averaged them across trials. We found that while as expected, there was a significant CSD amplitude increase in the response to BF tones, there was no post-stimulus CSD amplitude increase related to inhibitory responses in any of the layers (Fig. 5, same examples as in Fig. 3B), despite the organized sink-source pattern apparent in the averaged CSD profiles (Fig. 3B). Post-stimulus CSD amplitude increase was significantly smaller in response to non-BF tones across all sites compared to CSD

amplitude increase in response to BF tones (inset in Fig. 5). Statistical comparison of pre- to post-stimulus CSD amplitudes (averaged across all layers) showed a significant increase in the case of BF responses in all sites (dependent *t*-test, $p < 0.01$), while in most cases no significant effects were found in the case of inhibitory responses (0/19 in InhibHi, 3/17 in InhibLo and 1/14 and 4/14 in the InhibHi&Lo group). This suggests that the mechanism of inhibitory responses seen in the averaged laminar profiles (Fig. 3B) is a modulation of ongoing neuronal activity, rather than increased net transmembrane current flow like in response to BF tones.

If indeed the mechanism of inhibitory responses is the reset of ongoing oscillatory activity as we suspect, this should be reflected by an increased post-stimulus phase coherence across trials (indexed by intertrial coherence – ITC) in frequency bands corresponding to the dominant ongoing oscillations in A1 (Lakatos et al., 2005b) in the absence of pre- to post-stimulus increase in CSD amplitude (Sayers et al., 1974; Makeig et al., 2004; Shah et al., 2004). From this point on we do not differentiate between the three inhibitory groups in the description of results, as none of the analyzed variables differed significantly between the groups ($p > 0.01$, Kruskal-Wallis test). Also, since CSD response amplitude was largest in the supragranular layers, and ongoing/stimulus related oscillations appear to be coherent across cortical layers under a wide range of experimental conditions (Lakatos et al., 2005b, 2008), we selected the supragranular electrode channel with largest post-stimulus activity for further analysis (white arrows in Fig. 3B). This selection is also justified by earlier findings showing that the excitability of a cortical column can be reliably linked to CSD oscillations in the supragranular layers (Lakatos et al., 2005b, 2007b, 2008).

To determine whether there was a stimulus related amplitude change in any of the frequency bands, following wavelet decomposition, amplitudes of the single trial responses were computed in several frequency bands ranging from 1 to 100 Hz. Time frequency maps in Figure 6A show an example for excitatory (BF) and inhibitory responses from a representative site. It is apparent that the BF tone causes a large amplitude increase across the entire spectrum except for the low delta frequencies, characteristic of an evoked type complex waveform. On the contrary, we did not find a non-BF tone related amplitude increase in any of the frequency bands; the poststimulus amplitude trace is almost an exact match to the prestimulus one. Comparison of the pre- and post-stimulus oscillatory amplitudes in 6 frequency bands (1–2.4 Hz; 2.4–4 Hz; 4–10 Hz; 10–15 Hz; 15–25 Hz; 25–60 Hz) revealed no significant post-stimulus amplitude change for any of the inhibitory responses (dependent *t*-test, $p < 0.01$).

Next we calculated intertrial coherence (ITC) values across the single trials in each experiment, to determine whether the inhibitory laminar pattern seen in the average CSD profiles was due to an event-related phase synchrony across trials. The value of ITC will be 1 in the extreme case if the oscillatory phase is the same in each trial, and it will be 0 if the oscillatory phase across trials is random. Figure 6B shows that while the supragranular response to the BF tone is characterized by high ITC values across a wide range of frequencies, typical of an evoked type waveform (Lakatos et al., 2007, 2009), the inhibitory response is associated with phase locking (non-random phase distribution across trials indexed by higher ITC values) in three distinct frequency bands, which are the dominant oscillations present in the ongoing (prestimulus) neuronal activity (Fig. 6A and Lakatos et al., 2005b, 2007). This provides further evidence that phase reset perturbs the phase of ongoing activity without radically changing its overall composition.

The poststimulus ITC peaks in the delta (1–4Hz), theta (4–10 Hz) and gamma (25–55 Hz) frequency ranges were detectable in all inhibitory responses, and statistical testing showed that they signaled non-random phase distribution in all cases (Rayleigh $p < 0.01$). The mean

ITC value was 0.49 (SD = 0.18) in the delta, 0.40 (SD = 0.14) in the theta and 0.34 (SD = 0.14) in the gamma band for 100 single trials on average (variation between number of trials across experiments was relatively small, SD = 9.2). As the boxplots in Figure 6B illustrate, there was no difference between the frequencies of ITC peaks in the delta, theta and gamma ranges between responses to BF tones and inhibitory responses ($p > 0.01$, Wilcoxon signed-rank test), which indicates that both types of responses result in the phase reset of dominant ongoing oscillations, even though this cannot be unambiguously shown in the case of BF responses because of the evoked type response that results in wideband ITC even in the absence of phase reset (Lakatos et al., 2009). Taken together, the above results show that responses to BF tones are mixed - evoked and phase reset - type, while the mechanism of inhibitory responses is predominantly oscillatory phase reset.

It is well documented that neuronal oscillations reflect rhythmic changes of excitability in neuronal ensembles (reviewed by Young and Eggermont, 2009). Thus, if the phase ongoing oscillations are reset to is dependent on the frequency of auditory stimuli, this would aid in sharpening the tuning of different frequency regions in A1. To examine this possibility, we decided to compare the post stimulus phase of reset oscillations in the dominant frequency bands for both BF tone related and inhibitory responses. To determine the post-stimulus time instant at which to evaluate oscillatory phases, we calculated the mean timing of the maximum gamma ITC peak across inhibitory responses (mean = 23.4 ms, SD = 6.6). Interestingly, we found that it was not significantly different from the timing of the mean maximal MUA inhibition (23.46 ms, see above).

Histograms in Figure 6C show post stimulus single trial phase distributions for delta, theta and gamma oscillations associated with excitatory (left) and inhibitory (right) responses for a representative recording site. In both response types, there is a clearly significant grouping of phases in each frequency band. It is also apparent that the mean phases of the post-stimulus oscillations (black dotted line on histogram) are significantly different. In fact oscillations in the BF and non-BF conditions are in counter-phase, with the exception of the delta band. In the case of BF tone stimulation, the phases are grouped before and around the negative peak of the oscillations ($\pm\pi$ in Fig. 6C&D), which has been shown to correspond to the high excitability phase of ongoing CSD oscillations at this laminar location (Lakatos et al., 2005b, 2007). Conversely, single trial oscillatory phases in the inhibitory response are clustered around the positive peak which corresponds to the low excitability phase of ongoing oscillations at this supragranular location. Figure 6D displays the distribution of pooled mean phases associated with excitatory ($n = 50$) and inhibitory responses ($n = 64$), which shows a similar pattern. There is significant non-uniform phase distribution of the mean phases in each frequency band in the case of responses related to BF tones around the high excitability phase (negative peak) of ongoing oscillations (Rayleigh s uniformity tests, $p < 0.01$). In the case of inhibitory responses only the mean theta phases show a significantly non-uniform distribution around the low-excitability phase (opposite to that in the excitatory responses). While there is also apparent grouping in the distribution of gamma phases opposite to gamma phases in the excitatory response, this did not prove to be significant (Rayleigh s uniformity tests, $p = 0.06$), possibly as a consequence of response onset variation.

Delta oscillations are somewhat special compared to higher frequency oscillations in these experiments, since their frequency overlaps the frequency of stimulus presentation in our paradigms (SOA = 624.5 ms corresponding to a presentation frequency of 1.6 Hz). This means that they can entrain to the presentation rate of auditory stimuli used in our suprathreshold tonotopy paradigm as we showed previously (Lakatos et al., 2005). To complicate matters, while in most experiments we used a tonotopy paradigm that consisted of a random stream of different frequency pure tones, in 14 of our 50 (28%) penetrations we

delivered each frequency tone to the subjects in a blocked design. Could this be a source of the seemingly random phase distribution observed in Figure 6D?

Figure 7A shows the mean delta phase distributions of excitatory and inhibitory responses for blocked and random streams of pure tones. It is apparent that in the blocked design, mean delta phases associated with inhibitory non-BF tones are opposite to mean delta phases associated with streams of BF tones, and are clustered around the low excitability phase. In contrast, in the remaining 36 experiments where pure tones were delivered in a random order, delta oscillations associated with BF and inhibitory stimuli both entrained to the high excitability phases in most cases (Fig 7A, right). The mean of the mean delta phases (black dotted lines in Figure 7A) were significantly different between excitatory and inhibitory responses in the blocked condition (Fisher s nonparametric test for the equality of circular means, $p < 0.01$). This means that, as the averaged supragranular waveforms in Figure 7B illustrate, in the case when stimulus streams are formed by pure tones of the same frequency, supragranular delta oscillations can entrain to BF and non-BF stimulus streams with opposing phases. However, if the rhythmic stimulus stream consists of unpredictable frequency stimuli in a wide frequency range, delta oscillations tend to entrain to the stimulus stream with their high excitability phases. Thus it seems likely that in the case of rhythmic stimuli that consist of a narrow frequency range, entrained delta oscillations act as rhythmical "filters" by enhancing responses to BF and suppressing responses to non-BF tones. We have to note, that the experiments that yielded the data for the present study were not specifically designed to distinguish between the effects of uniform and random frequency content in rhythmic stimulus streams on oscillatory entrainment. Further studies that parametrically vary the broadness of the frequency content and stimulation rate are needed to study the dynamics of this effect, and to decide whether delta oscillations are special in this regard.

Our finding that a phase difference (opposition) of neuronal oscillations in local neuronal ensembles can occur at distances as small as 1 mm – which corresponds to approximately an octave difference in tuning – across all the frequency ranges of the oscillatory spectrum investigated in the present study indicates that even low frequency (delta) oscillations can be fairly local. To further specify the characteristics of local neuronal oscillatory activity, one would have to record ongoing and event related neuronal activity at varying distances simultaneously across A1. We speculate that while ongoing oscillatory activity may be independent even at the scale of neighboring cortical columns (dimensions well under 0.5 mm), the independence of event related (phase reset) oscillatory activity is restricted by the selectivity of non-specific thalamocortical inputs, which are known to project more widely than lemniscal inputs.

## DISCUSSION

In the present study, we found that about 80% of A1 sites respond with significant MUA suppression to pure tones with frequencies that differ from their preferred frequency (BF). Analysis of MUA and concomitant CSD laminar response profiles in these sites revealed that BF tones produced a strong activation of all cortical layers with an initial postsynaptic response (current sink with concomitant increase in action potentials) in the granular layer, followed by later responses in extragranular layers, typical of an excitatory "feedforward" or "driving" type activation profile (Schroeder et al 2003; Lakatos et al., 2007). On the other hand non-BF inhibitory tones produced a weaker CSD response characterized by a simultaneous activation of all cortical layers, suggesting – similar to granular layers – a direct activation of supragranular layers. In addition, the arrangement of sinks and sources was inverted in the laminar profiles of inhibitory responses relative to BF responses. Single trial time frequency analysis of the event-related oscillations revealed that – at least in the

supragranular layers – responses associated with non-BF inhibitory tones were most likely a result of phase resetting of ongoing oscillations within specific frequency bands. We also found that while in the mixed evoked-phase reset type responses to BF tones, oscillations are reset to high excitability phases, in response to non-BF tones, ongoing oscillatory activity is generally reset to opposing, low excitability phases.

### Prevalence of Inhibition in Primary Auditory Cortex

We found that 14 out of 64 A1 sites (22%) investigated in the present study did not show a significant post stimulus MUA suppression to any of the pure tones presented. Even though we did not find a significant post-stimulus inhibition in these sites, responses to pure tones whose frequency was about 2 octaves away from the BF showed the smallest, in most cases slightly below baseline post-stimulus MUA. A potential reason why we did not find MUA suppression in all A1 sites investigated is that attention was not engaged during the presentation of the stimuli. Since it has been shown that the phase reset of ongoing oscillatory activity is strongly dependent on stimulus salience (Lakatos et al., 2009), it is likely that if auditory stimuli were made task-relevant, this would result in stronger phase reset. Our finding that the phase to which ongoing oscillations are reset to depends on the stimulus frequency predicts that both inhibition and excitation would be facilitated under attentive listening conditions, resulting in sharper tuning. Since in our experiments attention was not directly manipulated, it remains to be tested in behaving animals attending to specific frequencies whether the common finding that frequency tuning in auditory cortex can be modified by attention (e.g. Fritz et al., 2003, 2005; Bidet-Caulet et al., 2007; Kauramaki et al., 2007; Okamoto et al., 2007) is due to this mechanism.

Similar to prior studies, our results demonstrate that inhibitory sideband asymmetry depends on the BF, which was suggested to underlie the topographic organization of FM direction selectivity in primary auditory cortex (Zhang et al., 2003). In addition to an opposite direction sideband asymmetry, another difference between sites with low and high BFs is that while in sites with low BFs, inhibition to high frequency sounds is "complete", sites with high BF tend to respond with a short excitation to low frequency sounds before the inhibitory response. This could be simply an 'artifact' of the different response onset latencies related to low and high frequency stimuli (discussed below), but it could also serve an important role in the perception of spectrally complex stimuli, like species specific communication or speech. If true, this would indicate that similar to functional differences along the isofrequency axis (e.g. Middlebrooks et al., 1980; Cheung et al., 2001; Read et al., 2002), functional differences also exist along the tonototopic axis in primary auditory cortex.

### Mechanisms of Inhibitory Responses

Our results show that while the excitation driven by the BF tone occurs earlier in the granular than in the supragranular layers indicating a sequential laminar activation, non BF tone-related inhibition occurs simultaneously across the layers, suggesting parallel activation. This indicates that – at least initially – granular and supragranular inhibition might occur via different routes and mechanisms, which we will first discuss separately beginning with the granular layer.

We found that similar to excitatory responses, inhibitory response onsets to pure tones also depend on their frequency, and that in general, inhibitory response onset to a given pure tone is about 3–4 ms later than excitatory response to the same frequency tone in the granular layer in both MUA and CSD profiles (Figures 2 & 4), which parallels the delay between excitation and inhibition reported by Wehr and Zador, (2003). This suggests that the mechanism of initial granular layer MUA suppression is feedforward inhibition via specific

TC afferents, and the delay is due to the disynaptic nature of the inhibition, as opposed to the monosynaptic excitatory response. (Swadlow, 2002; Wehr and Zador, 2003; Zhang et al., 2003; Tan et al., 2004; Cruikshank et al., 2007; Wu et al., 2008).

How can this mechanism explain that while – as expected based on the delay of inhibition compared to excitation – there is always a short excitation preceding inhibition at high frequency A1 sites, inhibition to high frequency tones in low frequency sites completely abolishes excitation? A key observation in this regard is that the difference between the onset of excitation and suppression is on the scale of the difference between the onset of responses to different frequency BF tones. Another pre-requisite for this finding is that excitation and inhibition are mediated by TC afferents from different frequency regions of the MGNv. One way this is possible is if inhibitory receptive fields in A1 are broader than excitatory ones, like in primary somatosensory cortex (Swadlow, 2002). High intensity pure tones, like the ones used in the present study will activate a considerably broad area of the cochlear receptor surface around the region corresponding to the pure tone frequency, which will activate TC afferents in a relatively wide frequency band (Aitkin and Webster, 1972). While specific feedforward (layer 4) activation of the excitatory neurons in a given area is mediated by TC neurons that match the BF of the site, suppression is mediated through TC afferents tuned to other frequencies as well. Therefore, if suppression is activated by TC afferents that are tuned to higher frequencies and thus are activated faster, this suppression can completely prevent weaker excitatory responses mediated by lower frequency TC afferents that are 'slower'.

To summarize, our results confirm that feedforward inhibition in primary auditory cortex is more broadly tuned than excitation (Wu et al., 2008), and this results in characteristic interactions of excitation and inhibition in the neuronal ensemble responses to non-BF tones that is dependent on the frequency relation of the non-BF tone to the BF. In theory, the broader tuning of inhibitory cell populations could be mediated by a slightly different, more divergent set of TC inputs than those mediating excitation, similar to the suggested TC connectivity of the barrel cortex (Swadlow, 2002), however a recent study in primary auditory cortex found that the frequency range of TC inputs is similar between excitatory (regular spiking) and inhibitory (fast spiking) neurons (Wu et al., 2008). Thus, the broader tuning of feedforward inhibition that results in the lateral sharpening of frequency tuning is likely due to less selective outputs: inhibitory neurons are capable of converting a broader range of synaptic input into action potentials than excitatory ones (Cruikshank et al., 2007).

In a recent study, Atencio and Schreiner (2010) found that interlaminar differences in temporal and spectral modulation transfer functions in A1 cannot be explained by a purely sequential interlaminar flow of information, thus suggesting the influence of non-lemniscal thalamocortical and/or horizontal inputs on auditory stimulus processing in A1 cortical columns. Our results also make the case for this, since we found that response onset latency to non-BF tones is not significantly different in the granular and supragranular layers, thus they are not activated sequentially like in the case of typical feedforward type responses to BF tones. A second potential route would be activation through horizontal intracortical inhibitory (Tomioka et al., 2005) or excitatory (Kurt et al., 2008) connections. However, if we consider, that in cases where inhibition occurs to higher frequency tones than the BF, response onset in the supragranular layers is the same to BF and non-BF tones (InhibHi and InhibHiLo2 in Figure 4), then this route seems unlikely, since it should result in a more significant delay of the non-BF compared to the BF response onset (even if we consider that response onset to a 2 octave higher tone would be approximately 2 ms earlier, resulting in an earlier activation of horizontal fibers). Thus, the most likely candidate is the third possible route which is activation of the supragranular layers by non-specific (non-lemniscal) TC afferents. This "activation" as our study revealed results in the frequency specific reset of

ongoing neuronal activity through afferents that most likely originate in the medial region of the MGN, since it has been shown that these "non-specific" thalamic afferents target mainly supragranular neuronal ensembles (Roger and Arnault, 1989; Hashikawa et al., 1991; Molinari et al., 1995; Jones et al., 1998; Huang and Winer, 2000).

We can only speculate about the mechanism that enables frequency specificity of the phase (high vs. low excitability) ongoing oscillations are reset to. We think that this mechanism is most likely thalamic, for the reason that the thalamus seems to be a better strategic location to orchestrate the coherent activity of neuronal populations across A1 than an intracortical mechanism. We also speculate that switching between an excitatory and inhibitory type phase reset in response to different frequency tones might involve the reticular nucleus of the thalamus (TRN) since this structure is the major source of inhibition to the MGN (Guillery et al., 1998; Crabtree, 1998). If this would be the case, the rich connections of the TRN with prefrontal cortical areas (Zikopoulos and Barbas, 2006) could explain how top-down influences are able to modulate the strength of oscillatory phase reset (Lakatos et al., 2009).

New techniques, such as the lentivirus mediated expression of photosensitive ion channels (e.g. Cruikshank et al., 2010) selectively in non-specific thalamocortically projecting neurons might provide invaluable information about the anatomical substrates of oscillatory phase reset of sensory oscillations in the near future. Selective pharmacological silencing of intracortical activity in a given A1 region (with the $GABA_A$ receptor agonist muscimol, similar to Happel et al., 2010) could also help to disentangle the contribution of horizontal and non-specific thalamocortical inputs in responses to non-BF tones. We suggest that to achieve this, one would have to selectively silence a region of A1 where a given pure tone results in evoked type (lemniscal) activity, and record the neuronal activity of an A1 site that is unaffected by the muscimol effect. The reason for this is that a complete muscimol blockade of A1 would eliminate intracortically evoked activity, but would also abolish ongoing neuronal oscillations, thus oscillatory phase reset. In contrast, the selective silencing of the A1 region receiving lemniscal activation in response to a given frequency pure tone would effectively block the spread of "specific activity", while still enabling modulation of cortical activity through non-specific thalamocortical inputs in regions unaffected by pharmacological manipulation.

It is important to note that while oscillatory phase reset is most prevalent in the supragranular layers, the phase of ongoing supragranular oscillations reflects excitability changes in all laminae of cortical processing units (Lakatos et al., 2005, 2007, 2008). This is illustrated by Figure 8, which shows the phase triggered (grey arrows) averages of spontaneous CSD for two A1 sites. To facilitate comparison to the 'real' inhibitory responses, these sites are the same as in Figure 3, and we created a 'baseline' from randomly selected spontaneous epochs. The corresponding laminar MUA profiles show a remarkable similarity to the 'real' inhibitory responses, clearly establishing the possibility that inhibitory responses can emerge as a result of pure phase resetting of neuronal oscillations. Of note is that the MUA 'suppression' related to the low excitability phase of ongoing oscillations is largest in the granular layer compared to MUA related to random ongoing activity (baseline), and the MUA amplitude change appears cyclically fluctuating, just as it occurs in the inhibitory responses that we directly measured at these sites. In both cases there are two MUA suppression peaks, one at stimulus onset and one around 100 ms separated by a time period where MUA seems to return to baseline, suggesting a cyclical modulation around 10 Hz, which roughly corresponds to the wavelength of the dominant theta oscillation that is reset by auditory inputs.

These considerations suggest that while – for reasons detailed above – there is undoubtedly an initial inhibitory component related to specific feedforward TC pathways, the bulk of the inhibitory response, especially that following the early part of the response, is due to the phase reset of ongoing supragranular oscillations in A1. Selective blockade of non-specific thalamocortical inputs could provide definitive proof for this hypothesis. Note that even though we used the lower supragranular electrode site to 'trigger' epochs of spontaneous activity at specific phases of ongoing (Fig. 8), a sink-source pattern can be seen throughout all cortical laminae, indicating that CSD activity across the cortex is – at least to some degree – coherent or coupled to each other, as suggested by previous studies (e.g. Sakata and Harris 2009). Even the related MUA across all layers is either enhanced or suppressed simultaneously. Resetting cortical oscillations to a low excitability phase (present data) can aid specific feed forward inhibition and temporally extend its effects by lowering the membrane potential of excitatory neuronal populations, thereby tilting the balance of concurrently occurring specific TC input generated excitatory/inhibitory processes towards inhibition, and effectively preventing an excitatory response.

The intriguing finding that delta oscillations entrained differently to rhythmically presented stimulus streams based on the composition of the streams (narrow vs. wideband frequency content) indicates that concurrent with stimulus selection (Lakatos et al., 2008), entrained slow oscillations might play an important role in auditory stream segregation. Our results indicate the reset and entrainment of ongoing oscillatory activity by auditory inputs can be frequency specific, we propose that neuronal oscillations in A1 can "track" frequency and timing in attended auditory streams simultaneously. By arranging high excitability phases to coincide with key events in attended stimulus streams in both frequency (across A1) and time, attended streams get amplified and segregated along the two arguably most fundamental organizing dimensions in auditory processing. As a "bonus", streams that do not closely match either in frequency or time get suppressed by the low excitability phase of the entrained oscillations. To achieve this, oscillations would have to be simultaneously orchestrated (via phase reset and entrainment) across A1 by frequency specific inputs, which could be verified by multiple site recordings across A1.

### Conclusions

Our findings outline a dual mechanism of inhibition in A1. While one mechanism is mediated by specific, lemniscal thalamocortical inputs targeting layer 4, the other involves non-specific thalamocortical inputs targeting the supragranular layers. This latter mechanism involving the phase reset of ongoing oscillations is more dynamic and, based on earlier studies, has the potential to change the strength and possibly even shift the tuning of local neuronal ensembles in A1. Along with modulating excitability locally, this dynamic overlay of ongoing oscillatory activity is an ideal candidate for the orchestration of neuronal activity across A1 when processing complex auditory scenes.

## EXPERIMENTAL PROCEDURES

We analysed electrophysiological data recorded during 64 penetrations of area A1 of the auditory cortex of 9 macaques (*Macaca mulatta*), who had been prepared surgically for chronic awake electrophysiological recordings. No monkeys were used exclusively for this study; rather, they were all assigned to other primary experiments. Because all of our auditory cortex experiments require functional identification of recording sites using a battery of pure tone and broadband noise stimuli (see below), the data generated by these routine methodological procedures were available for the analyses described in the current study. The subjects were kept in an alert state during the recordings by interacting with them in the breaks between stimulus blocks, however, they were not required to attend or respond to the auditory stimuli. Laminar profiles of field potentials (EEG) and concomitant

population action potentials (multiunit activity or MUA) were obtained using linear array multi-contact electrodes (24 contacts, 100 μm intercontact spacing). One-dimensional current source density (CSD) profiles were calculated from the local field potential profiles using a three-point formula for estimation of the second spatial derivative of voltage.

The auditory stimuli presented through free field speakers were 7 different frequency pure tones ranging from 500 to 32000 kHz in one octave steps in separate blocks (14 out of 50 experiments), or a pseudorandom train of 14 different frequency pure tones ranging from 353.5Hz to 32kHz in half octave steps, and a broadband noise burst (BBN) at 60 dB SPL (duration: 100 ms, r/f time: 4 ms, ISI = 767, n = 1400). After selective averaging of the CSD and MUA responses to the different frequency pure tones and BBN, we determined the best frequency (BF) of the recording site. Utilizing the BF-tone related laminar CSD profile, the functional identification of the supragranular, granular and infragranular cortical layers in area A1 is straightforward based on our earlier studies (see Fig. 3B) (Schroeder et al., 1998;Lakatos et al., 2005a,2007).

For quantitative analysis of event related MUA amplitudes, the electrode contact with the largest BF tone-related MUA was selected, which was found to always reside in the granular layer (red trace in Fig. 1A). To determine if a site displayed significant inhibition, single trial mean MUA amplitudes were calculated for the 15 – 40ms time window (the transient part of the responses, Steinschneider et al., 2008) on this channel, and compared to the baseline (−50 – 0ms) (dependent t-test, $p < 0.01$). To determine MUA response onset latencies, the same granular electrode was used and response onset was defined as the earliest significant (> 2 standard deviation units) deviation of the averaged waveforms from their baseline (−50 – 0 ms), that was maintained for at least 5 ms. In the case of inhibitory responses, the onset of inhibition was determined by only taking negative direction MUA changes into account. The analysis of CSD onset latencies (Fig. 4) was performed similarly on two selected channels, one from supragranular and one from the granular layers. These electrode channels were selected based on which site had the largest amplitude sink in these layers in response to BF tones. When determining the onset of inhibitory responses, we only considered positive data points (sources, that can reflect net outward transmembrane current) in the 0–30 ms post-stimulus time interval. In 8 sites (from the InhibLo (n = 4) and InhibHi&Lo (n = 4) groups), CSD activity did not reach a significantly above baseline level in the 0–30 ms time interval, thus the inhibitory response onset could not be determined.

To extract auditory event related CSD amplitudes (Fig. 5), we calculated the analytic amplitude of the single trial CSD signals for the entire pass-band using the Hilbert transform. To statistically evaluate whether stimulus related responses resulted in a difference between pre- and post-stimulus CSD amplitude, we averaged the single trial analytic CSD amplitude across all cortical layers, and then compared these variables averaged in the pre-stimulus (−50–0 ms) and post-stimulus (0–50 ms) time intervals within experiments using dependent *t*-tests ($p < 0.01$). To create the phase triggered averages of spontaneous CSD and concomitant MUA in Figure 8, in non-overlapping 2 second segments of spontaneous activity we determined the time points that most closely corresponded to the combination of mean delta, theta and gamma oscillatory phases measured in real inhibitory responses (e.g. Fig 6C). Designating these time-points as 'triggers' (arrows in Fig. 8), we created 100 epochs from the spontaneous CSD and concomitant MUA and averaged them. To simulate a baseline where oscillatory phase is random, we also created 100 epochs ending at randomly selected time-points from the same spontaneous CSD and MUA recordings, and attached these epochs in front of the phase triggered ones (CSD and MUA preceding the arrows in Fig. 8).

Details of the surgery, electrophysiology and data analysis are described in the Supplemental Information.

## Supplementary Material

Refer to Web version on PubMed Central for supplementary material.

## Acknowledgments

Support for this work was provided by NIH grant R21 DC010415 from NIDCD, and NIMH grants MH061989 and MH060358.

## References

Aitkin LM, Webster WR. Medial geniculate body of the cat: organization and responses to tonal stimuli of neurons in ventral division. J Neurophysiol 1972;35:365–380. [PubMed: 5029955]

Atencio CA, Schreiner CE. Laminar diversity of dynamic sound processing in cat primary auditory cortex. J Neurophysiol 2010;103:192–205. [PubMed: 19864440]

Bidet-Caulet A, Fischer C, Besle J, Aguera PE, Giard MH, Bertrand O. Effects of selective attention on the electrophysiological representation of concurrent sounds in the human auditory cortex. J Neurosci 2007;27:9252–9261. [PubMed: 17728439]

Brugge JF, Merzenich MM. Responses of neurons in auditory cortex of the macaque monkey to monaural and binaural stimulation. J Neurophysiol 1973;36:1138–1158. [PubMed: 4761724]

Cheung SW, Bedenbaugh PH, Nagarajan SS, Schreiner CE. Functional organization of squirrel monkey primary auditory cortex: responses to pure tones. J Neurophysiol 2001;85:1732–1749. [PubMed: 11287495]

Crabtree JW. Organization in the auditory sector of the cat's thalamic reticular nucleus. J Comp Neurol 1998;390:167–182. [PubMed: 9453662]

Creutzfeldt O, Hellweg FC, Schreiner C. Thalamocortical transformation of responses to complex auditory stimuli. Exp Brain Res 1980;39:87–104. [PubMed: 6247179]

Cruikshank SJ, Lewis TJ, Connors BW. Synaptic basis for intense thalamocortical activation of feedforward inhibitory cells in neocortex. Nat Neurosci 2007;10:462–468. [PubMed: 17334362]

Cruikshank SJ, Urabe H, Nurmikko AV, Connors BW. Pathway-specific feedforward circuits between thalamus and neocortex revealed by selective optical stimulation of axons. Neuron 2010;65:230–245. [PubMed: 20152129]

Ferster D. Spatially opponent excitation and inhibition in simple cells of the cat visual cortex. J Neurosci 1988;8:1172–1180. [PubMed: 3357015]

Foeller E, Vater M, Kossl M. Laminar analysis of inhibition in the gerbil primary auditory cortex. J Assoc Res Otolaryngol 2001;2:279–296. [PubMed: 11669400]

Fritz J, Shamma S, Elhilali M, Klein D. Rapid task-related plasticity of spectrotemporal receptive fields in primary auditory cortex. Nat Neurosci 2003;6:1216–1223. [PubMed: 14583754]

Fritz J, Elhilali M, Shamma S. Active listening: task-dependent plasticity of spectrotemporal receptive fields in primary auditory cortex. Hear Res 2005;206:159–176. [PubMed: 16081006]

Galindo-Leon EE, Lin FG, Liu RC. Inhibitory plasticity in a lateral band improves cortical detection of natural vocalizations. Neuron 2009;62:705–716. [PubMed: 19524529]

Guillery RW, Feig SL, Lozsadi DA. Paying attention to the thalamic reticular nucleus. Trends Neurosci 1998;21:28–32. [PubMed: 9464683]

Happel MF, Jeschke M, Ohl FW. Spectral integration in primary auditory cortex attributable to temporally precise convergence of thalamocortical and intracortical input. J Neurosci 2010;30:11114–11127. [PubMed: 20720119]

Hashikawa T, Rausell E, Molinari M, Jones EG. Parvalbumin- and calbindin-containing neurons in the monkey medial geniculate complex: differential distribution and cortical layer specific projections. Brain Res 1991;544:335–341. [PubMed: 2039948]

Horikawa J, Hosokawa Y, Kubota M, Nasu M, Taniguchi I. Optical imaging of spatiotemporal patterns of glutamatergic excitation and GABAergic inhibition in the guinea-pig auditory cortex in vivo. J Physiol 1996;497(Pt 3):629–638. [PubMed: 9003549]

Huang CL, Winer JA. Auditory thalamocortical projections in the cat: laminar and areal patterns of input. J Comp Neurol 2000;427:302–331. [PubMed: 11054695]

Jones EG. Viewpoint: the core and matrix of thalamic organization. Neuroscience 1998;85:331–345. [PubMed: 9622234]

Kaas JH. Topographic maps are fundamental to sensory processing. Brain Res Bull 1997;44:107–112. [PubMed: 9292198]

Kaas JH, Hackett TA. Subdivisions of auditory cortex and processing streams in primates. Proc Natl Acad Sci U S A 2000;97:11793–11799. [PubMed: 11050211]

Kaur S, Lazar R, Metherate R. Intracortical pathways determine breadth of subthreshold frequency receptive fields in primary auditory cortex. J Neurophysiol 2004;91:2551–2567. [PubMed: 14749307]

Kauramaki J, Jaaskelainen IP, Sams M. Selective attention increases both gain and feature selectivity of the human auditory cortex. PLoS One 2007;2:e909. [PubMed: 17878944]

Kosaki H, Hashikawa T, He J, Jones EG. Tonotopic organization of auditory cortical fields delineated by parvalbumin immunoreactivity in macaque monkeys. J Comp Neurol 1997;386:304–316. [PubMed: 9295154]

Krukowski AE, Miller KD. Thalamocortical NMDA conductances and intracortical inhibition can explain cortical temporal tuning. Nat Neurosci 2001;4:424–430. [PubMed: 11276234]

Kurt S, Deutscher A, Crook JM, Ohl FW, Budinger E, Moeller CK, Scheich H, Schulze H. Auditory cortical contrast enhancing by global winner-take-all inhibitory interactions. PLoS One 2008;3:e1735. [PubMed: 18320054]

Lakatos P, Pincze Z, Fu KM, Javitt DC, Karmos G, Schroeder CE. Timing of pure tone and noise-evoked responses in macaque auditory cortex. Neuroreport 2005A;16:933–937. [PubMed: 15931064]

Lakatos P, Shah AS, Knuth KH, Ulbert I, Karmos G, Schroeder CE. An oscillatory hierarchy controlling neuronal excitability and stimulus processing in the auditory cortex. J Neurophysiol 2005B;94:1904–1911. [PubMed: 15901760]

Lakatos P, Chen CM, O'Connell MN, Mills A, Schroeder CE. Neuronal oscillations and multisensory interaction in primary auditory cortex. Neuron 2007;53:279–292. [PubMed: 17224408]

Lakatos P, Karmos G, Mehta AD, Ulbert I, Schroeder CE. Entrainment of neuronal oscillations as a mechanism of attentional selection. Science 2008;320:110–113. [PubMed: 18388295]

Lakatos P, O'Connell MN, Barczak A, Mills A, Javitt DC, Schroeder CE. The leading sense: supramodal control of neurophysiological context by attention. Neuron 2009;64:419–430. [PubMed: 19914189]

Lee CC, Schreiner CE, Imaizumi K, Winer JA. Tonotopic and heterotopic projection systems in physiologically defined auditory cortex. Neuroscience 2004;128:871–887. [PubMed: 15464293]

Liu BH, Wu GK, Arbuckle R, Tao HW, Zhang LI. Defining cortical frequency tuning with recurrent excitatory circuitry. Nat Neurosci 2007;10:1594–1600. [PubMed: 17994013]

Makeig S, Debener S, Onton J, Delorme A. Mining event-related brain dynamics. Trends Cogn Sci 2004;8:204–210. [PubMed: 15120678]

Mendelson JR, Schreiner CE, Sutter ML. Functional topography of cat primary auditory cortex: response latencies. J Comp Physiol A 1997;181:615–633. [PubMed: 9449822]

Merzenich MM, Brugge JF. Representation of the cochlear partition of the superior temporal plane of the macaque monkey. Brain Res 1973;50:275–296. [PubMed: 4196192]

Middlebrooks JC, Dykes RW, Merzenich MM. Binaural response-specific bands in primary auditory cortex (AI) of the cat: topographical organization orthogonal to isofrequency contours. Brain Res 1980;181:31–48. [PubMed: 7350963]

Miller LM, Escabi MA, Read HL, Schreiner CE. Functional convergence of response properties in the auditory thalamocortical system. Neuron 2001;32:151–160. [PubMed: 11604146]

Miller LM, Escabi MA, Read HL, Schreiner CE. Spectrotemporal receptive fields in the lemniscal auditory thalamus and cortex. J Neurophysiol 2002;87:516–527. [PubMed: 11784767]

Mitzdorf U. Current source-density method and application in cat cerebral cortex: investigation of evoked potentials and EEG phenomena. Physiol Rev 1985;65:37–100. [PubMed: 3880898]

Moeller CK, Kurt S, Happel MF, Schulze H. Long-range effects of GABAergic inhibition in gerbil primary auditory cortex. Eur J Neurosci 2010;31:49–59. [PubMed: 20092555]

Molinari M, Dell'Anna ME, Rausell E, Leggio MG, Hashikawa T, Jones EG. Auditory thalamocortical pathways defined in monkeys by calcium-binding protein immunoreactivity. J Comp Neurol 1995;362:171–194. [PubMed: 8576432]

Okamoto H, Stracke H, Wolters CH, Schmael F, Pantev C. Attention improves population-level frequency tuning in human auditory cortex. J Neurosci 2007;27:10383–10390. [PubMed: 17898210]

Read HL, Winer JA, Schreiner CE. Functional architecture of auditory cortex. Curr Opin Neurobiol 2002;12:433–440. [PubMed: 12139992]

Recanzone GH, Schreiner CE, Merzenich MM. Plasticity in the frequency representation of primary auditory cortex following discrimination training in adult owl monkeys. J Neurosci 1993;13:87–103. [PubMed: 8423485]

Roger M, Arnault P. Anatomical study of the connections of the primary auditory area in the rat. J Comp Neurol 1989;287:339–356. [PubMed: 2778109]

Sakata S, Harris KD. Laminar structure of spontaneous and sensory-evoked population activity in auditory cortex. Neuron 2009;64:404–418. [PubMed: 19914188]

Sayers BM, Beagley HA, Henshall WR. The mechansim of auditory evoked EEG responses. Nature 1974;247:481–483. [PubMed: 4818547]

Scholl B, Gao X, Wehr M. Nonoverlapping sets of synapses drive on responses and off responses in auditory cortex. Neuron 2010;65:412–421. [PubMed: 20159453]

Schroeder CE, Mehta AD, Givre SJ. A spatiotemporal profile of visual system activation revealed by current source density analysis in the awake macaque. Cereb Cortex 1998;8:575–592. [PubMed: 9823479]

Schroeder CE, Smiley J, Fu KG, McGinnis T, O'Connell MN, Hackett TA. Anatomical mechanisms and functional implications of multisensory convergence in early cortical processing. Int J Psychophysiol 2003;50:5–17. [PubMed: 14511832]

Schroeder CE, Lakatos P. Low-frequency neuronal oscillations as instruments of sensory selection. Trends Neurosci 2009;32:9–18. [PubMed: 19012975]

Shah AS, Bressler SL, Knuth KH, Ding M, Mehta AD, Ulbert I, Schroeder CE. Neural dynamics and the fundamental mechanisms of event-related brain potentials. Cereb Cortex 2004;14:476–483. [PubMed: 15054063]

Shamma SA, Symmes D. Patterns of inhibition in auditory cortical cells in awake squirrel monkeys. Hear Res 1985;19:1–13. [PubMed: 4066511]

Steinschneider M, Fishman YI, Arezzo JC. Spectrotemporal analysis of evoked and induced electroencephalographic responses in primary auditory cortex (A1) of the awake monkey. Cereb Cortex 2008;18:610–625. [PubMed: 17586604]

Suga N. Sharpening of frequency tuning by inhibition in the central auditory system: tribute to Yasuji Katsuki. Neurosci Res 1995;21:287–299. [PubMed: 7777219]

Sutter ML, Schreiner CE, McLean M, O'connor KN, Loftus WC. Organization of inhibitory frequency receptive fields in cat primary auditory cortex. J Neurophysiol 1999;82:2358–2371. [PubMed: 10561411]

Swadlow HA. Thalamocortical control of feed-forward inhibition in awake somatosensory 'barrel' cortex. Philos Trans R Soc Lond B Biol Sci 2002;357:1717–1727. [PubMed: 12626006]

Tan AY, Zhang LI, Merzenich MM, Schreiner CE. Tone-evoked excitatory and inhibitory synaptic conductances of primary auditory cortex neurons. J Neurophysiol 2004;92:630–643. [PubMed: 14999047]

Tanji K, Leopold DA, Ye FQ, Zhu C, Malloy M, Saunders RC, Mishkin M. Effect of sound intensity on tonotopic fMRI maps in the unanesthetized monkey. Neuroimage 2010;49:150–157. [PubMed: 19631273]

Tomioka R, Okamoto K, Furuta T, Fujiyama F, Iwasato T, Yanagawa Y, Obata K, Kaneko T, Tamamaki N. Demonstration of long-range GABAergic connections distributed throughout the mouse neocortex. Eur J Neurosci 2005;21:1587–1600. [PubMed: 15845086]

Wang J, Caspary D, Salvi RJ. GABA-A antagonist causes dramatic expansion of tuning in primary auditory cortex. Neuroreport 2000;11:1137–1140. [PubMed: 10790896]

Wehr M, Zador AM. Balanced inhibition underlies tuning and sharpens spike timing in auditory cortex. Nature 2003;426:442–446. [PubMed: 14647382]

Winer JA, Lee CC. The distributed auditory cortex. Hear Res 2007;229:3–13. [PubMed: 17329049]

Wu GK, Arbuckle R, Liu BH, Tao HW, Zhang LI. Lateral sharpening of cortical frequency tuning by approximately balanced inhibition. Neuron 2008;58:132–143. [PubMed: 18400169]

Young CK, Eggermont JJ. Coupling of mesoscopic brain oscillations: recent advances in analytical and theoretical perspectives. Prog Neurobiol 2009;89:61–78. [PubMed: 19549556]

Zhang LI, Tan AY, Schreiner CE, Merzenich MM. Topography and synaptic shaping of direction selectivity in primary auditory cortex. Nature 2003;424:201–205. [PubMed: 12853959]

Zikopoulos B, Barbas H. Prefrontal projections to the thalamic reticular nucleus form a unique circuit for attentional mechanisms. J Neurosci 2006;26:7348–7361. [PubMed: 16837581]

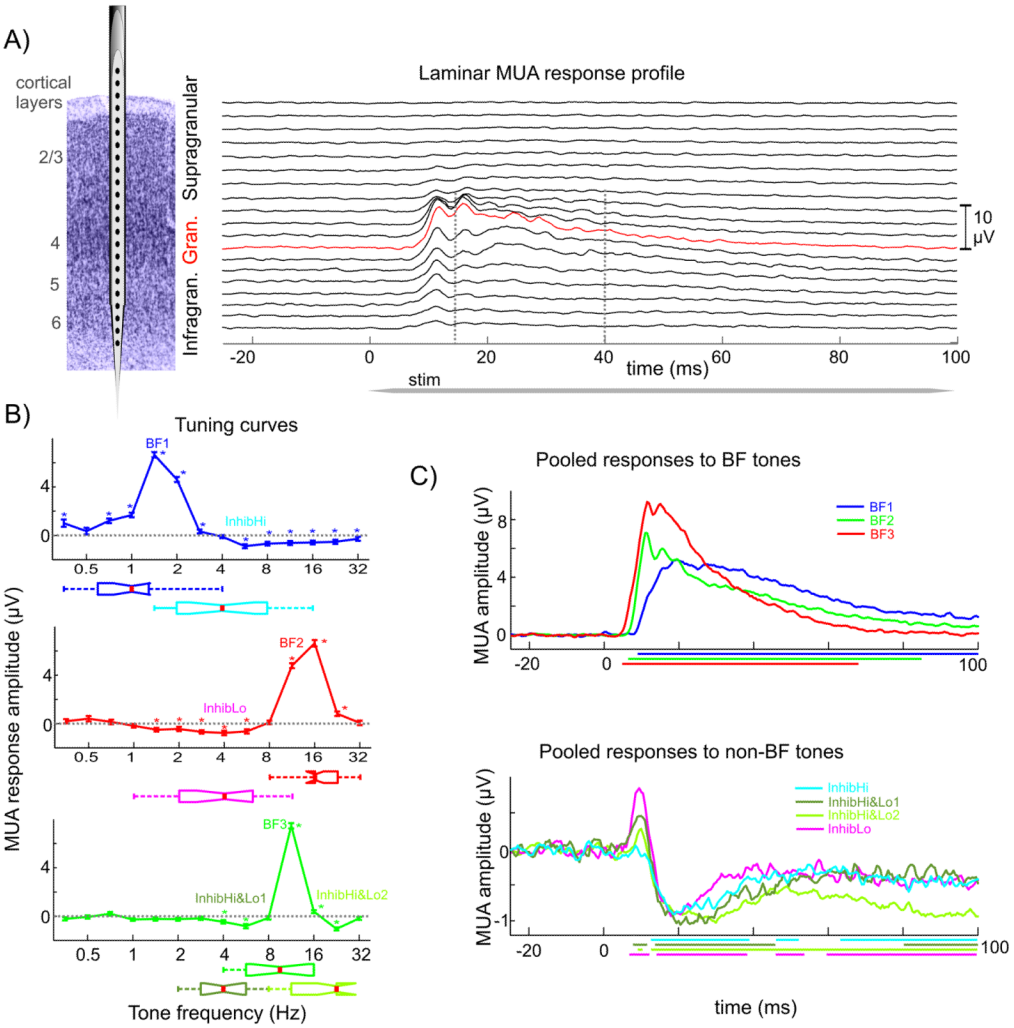


**Figure 1. Excitatory and inhibitory MUA responses**

**A)** On the left is a schematic of a linear array multielectrode positioned in primary auditory cortex. To the right is the laminar profile of averaged MUA in response to the BF tone in area A1. For quantitative analyses of the MUA response, the electrode contact with the largest MUA was selected (red trace). **B)** Frequency tuning curves for 3 representative A1 sites: one displaying an upper inhibitory sideband (blue, InhibHi), one a lower inhibitory sideband (red, InhibLo), and a third one both an upper and lower inhibitory sideband (green, InhibHi&Lo). Stars denote responses where MUA response amplitudes differ significantly from baseline. Box plots below show pooled frequencies of BF tones and non-BF tones that resulted in the largest inhibition across all sites that had similar tuning curves (InhibHi (n = 19), InhibLo (n = 17), and InhibHi&Lo (n = 14)). **C)** Averaged MUA responses to BF tones and non-BF tones that resulted in the largest inhibition. The grouping of sites is the same as in B). Colored lines below denote time intervals of significant post-stimulus MUA amplitude changes.

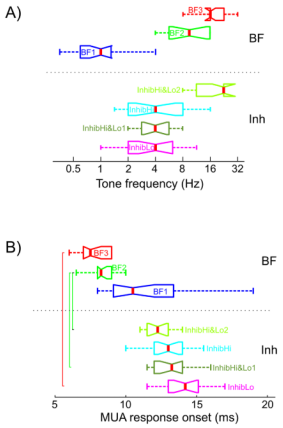


**Figure 2. The frequency dependence of granular MUA response onset**

**A)** Box and whisker plot shows the pooled frequency of tones that resulted in the largest excitatory (BF) and inhibitory responses. Grouping and nomenclature are the same as in Fig. 1B) & 1C). **B)** Pooled granular MUA onset latencies for the 3 BF groups (top) and the 4 non-BF inhibitory response groups (bottom). Brackets indicate where the onset latency of excitatory and inhibitory MUA response is significantly different across InhibHi, InhibLo, and InhibHi&Lo sites (Tukey's test, $p<0.01$).

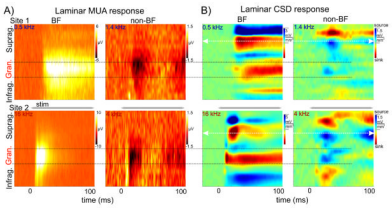


**Figure 3. MUA and current source density (CSD) profiles associated with BF and non-BF tones in A1**

**A)** MUA response profiles from a representative low BF (0.5 kHz, top) and high BF (16 kHz, bottom) site. MUA response profiles to non-BF tones (1.4 kHz and 4 kHz respectively) in the same sites display suppression which is largest in the granular layers. Note that inhibition seems to be fluctuating (two 'inhibitory' peaks, one at response onset and one around 100 ms). **B)** Concomitant CSD response profiles. Note that the laminar pattern of sink source pairs is reversed in response to non-BF tones when compared to BF responses. White arrows shows the supragranular channels with the largest amplitude sink in response to BF tones that were selected for further analyses in these sites.

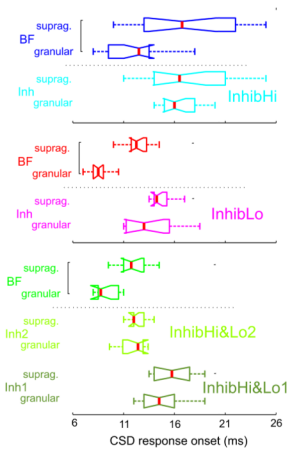


**Figure 4. Laminar CSD response onset in excitatory (BF) and inhibitory response profiles**

CSD response onset to BF and non-BF (inhibitory) tones in the supragranular and granular layers of InhibHi (n = 19), InhibLo (n = 13) and InhibHi&Lo (n = 10) sites. Brackets indicate significant differences between response onset latencies in the granular and supragranular layers (Wilcoxon signed rank test, $p<0.01$).

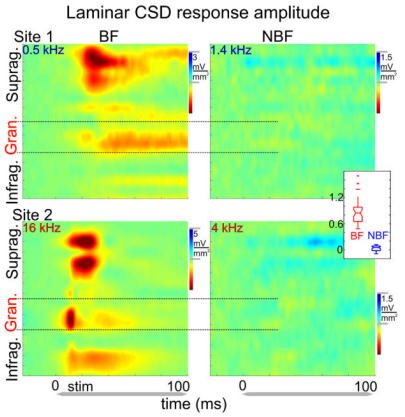


**Figure 5. CSD amplitude profiles**

Color maps show averaged single trial CSD amplitude profiles (calculated using the Hilbert transform), in response to BF and non-BF tones (same recordings as in Fig. 3B). The inset shows the average laminar post-stimulus CSD amplitude increase in all sites in response to BF (n = 50) and non-BF tones (n = 64).

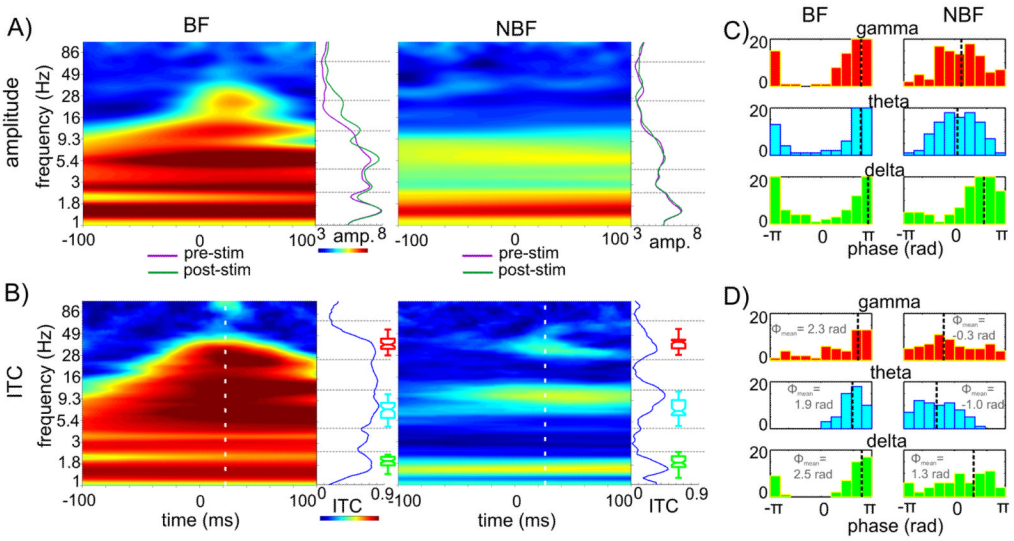


**Figure 6. Oscillatory properties of BF and non-BF responses**

**A)** Time-frequency maps show the average oscillatory amplitude of wavelet transformed single trials recorded at a supragranular electrode location in response to BF (left) and non-BF (right) tones. Traces to right of color maps show the pre- (purple) and post-stimulus (green) amplitudes (averaged in the −100 – 0 and 0 – 100 ms time-intervals respectively). **B)** Time-frequency plots show the inter trial coherence (ITC) for same recordings. White dotted line on color maps shows the time of the mean gamma ITC peak, blue traces to the right of color maps show the ITC values at this post-stimulus time instant. Boxplots display the pooled frequencies of delta (green), theta (cyan) and gamma (red) ITC peaks across all BF and non-BF sites. **C)** Histograms show single trial post stimulus delta, theta and gamma oscillatory phase distributions associated with BF (right) and non-BF (left) stimuli. Black dotted lines mark the angular mean of the single trial phases. **D)** Pooled delta, theta and gamma mean oscillatory phase distribution of all sites associated with BF and non-BF stimuli. Angular mean of the mean phases (marked by dotted lines) are inset.

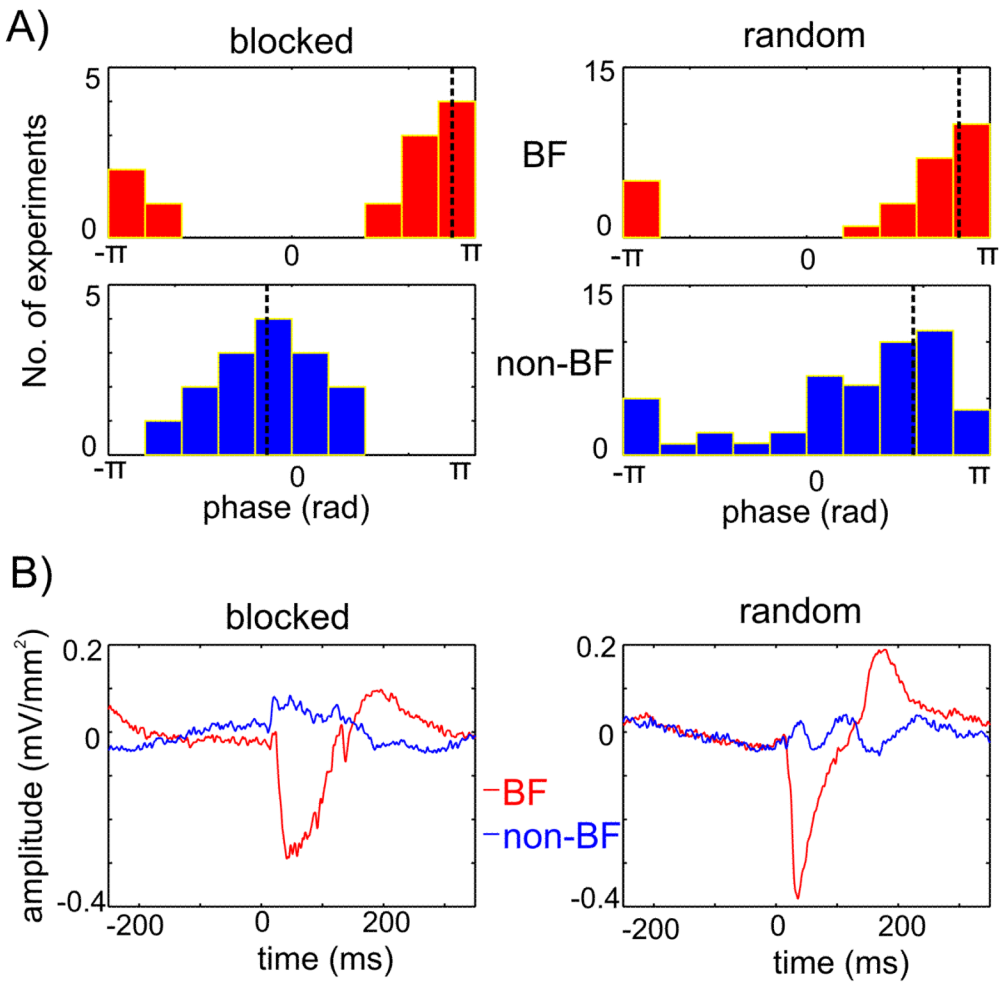


**Figure 7. Delta oscillatory entrainment**

**A)** The distribution of mean delta phases in response to BF (upper) and non-BF (lower) tones, for blocked (left, n=14) and random (right, n=36) streams of pure tones. Black dotted lines show the angular mean of the mean phases. **B)** Averaged supragranular CSD responses to BF (red) and non-BF (blue) pure tones from an experiment where different frequency pure tones were presented in separate blocks (blocked), and from an experiment where different frequency pure tones were presented randomly (random). Note the opposite sign low frequency pre-stimulus activity in the blocked case.

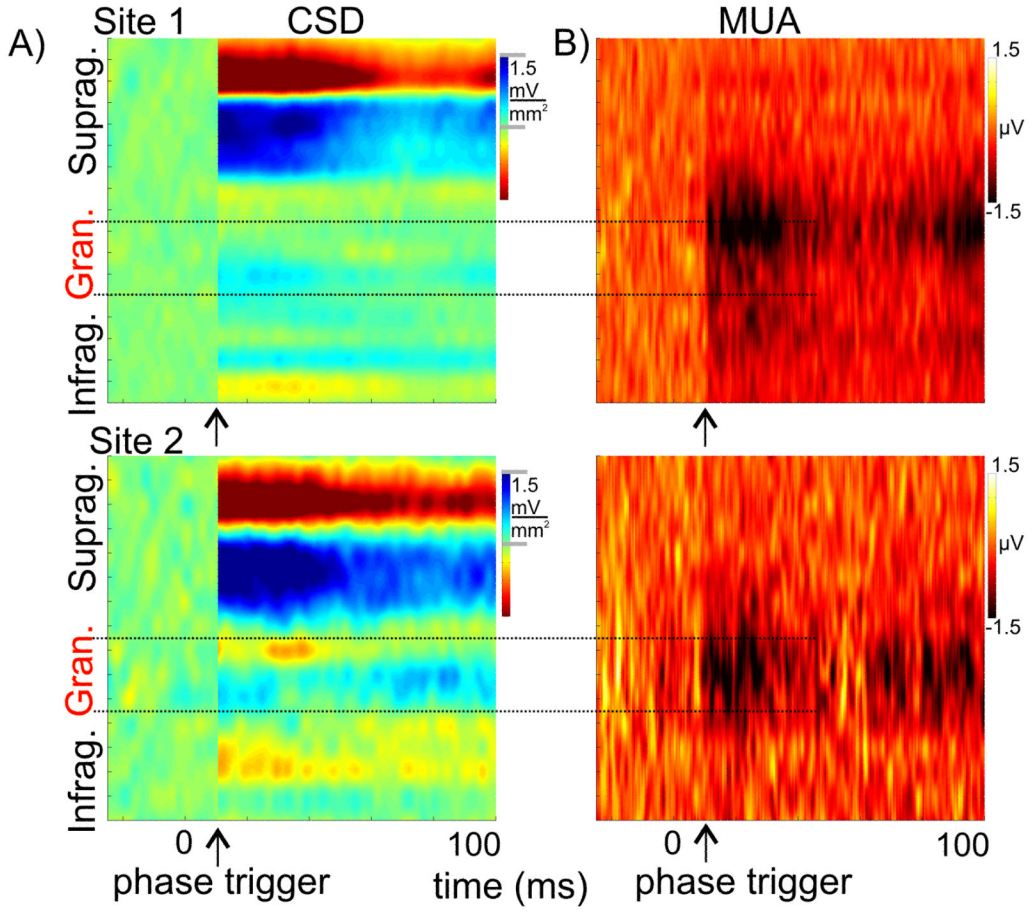


**Figure 8. Phase triggered averages of spontaneous CSD and concomitant recorded MUA**

**A)** The two phase triggered average profiles were created from sponataneous activity recorded in the same locations as CSD response profiles in Figures 3 & 5. The phase triggered profiles (starting at the arrow) are the average of epochs of ongoing activity triggered at phases of supragranular delta, theta and gamma oscillations that correspond to the mean phase of these oscillations in the inhibitory responses. The "baseline" (activity preceding the arrows) was created from averaging randomly selected epochs of ongoing activity. **B)** Laminar profiles of concomitant MUA